Heliyon 10 (2024) e33206

Contents lists available at ScienceDirect

Heliyon

journal homepage: www.cell.com/heliyon

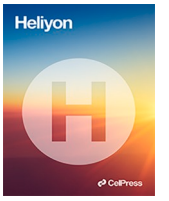

Research article

Comprehensive analysis and experimental verification reveal the molecular characteristics of EGLN3 in pan-cancer and its relationship with the proliferation and apoptosis of lung cancer

Yuan-Xiang Shi [a,*], Peng-Hui Dai [b], Tao Chen [c], Jian-Hua Yan [d]

[a] Institute of Clinical Medicine, Hunan Provincial People's Hospital, The First Affiliated Hospital of Hunan Normal University, Changsha, China
[b] Department of Pathology, Hunan Provincial People's Hospital, The First Affiliated Hospital of Hunan Normal University, Changsha, China
[c] School of Medicine, Hunan Normal University, Changsha, China
[d] Department of Cardiac Thoracic Surgery, Hunan Provincial People's Hospital, The First Affiliated Hospital of Hunan Normal University, Changsha, Hunan, China

ARTICLE INFO

Keywords:
EGLN3
Single-cell RNA sequencing
Tumor microenvironment
Cell apoptosis
Hypoxia

ABSTRACT

Background: Egl-9 family hypoxia-inducible factor 3 (EGLN3) is involved in the regulation of tumor microenvironment and tumor progression. However, its biological function and clinical significance in various cancers remain unclear.
Methods: RNA-seq, immunofluorescence, and single-cell sequencing were used to investigate the expression landscape of EGLN3 in pan-cancer. The TISCH2 and CancerSEA databases were used for single-cell function analysis of EGLN3 in tumors. TIMER2.0 database was used to explain the relationship between EGLN3 expression and immune cell infiltration. In addition, the LinkedOmics database was used to perform KEGG enrichment analysis of EGLN3 in pan-cancer. siRNA was used to silence gene expression. CCK8, transwell migration assay, flow cytometry analysis, RT-PCR, and western blotting were used to explore biological function of EGLN3.
Results: The results showed that EGLN3 was highly expressed in a variety of tumors, and was mainly localized to the cytosol. EGLN3 expression is associated with immunoinfiltration of a variety of immune cells, including macrophages in the tumor immune microenvironment and tumor-associated fibroblasts. Functional experiments revealed that EGLN3 knockdown could inhibit cell proliferation, migration, and promote cell apoptosis. In addition, we found that Bax expression was up-regulated and Bcl-2 expression was down-regulated in the si-EGLN3 group. Taken together, as a potential oncogene, EGLN3 is involved in the regulation of tumor malignant process, especially tumor cell apoptosis.
Conclusion: We comprehensively investigated the expression pattern, single-cell function, immune infiltration level and regulated signaling pathway of EGLN3 in pan-cancer. We found that EGLN3 is an important hypoxia and immune-related gene that may serve as a potential target for tumor immunotherapy.

* Corresponding author.
E-mail address: yuanxiangshi@hunnu.edu.cn (Y.-X. Shi).

https://doi.org/10.1016/j.heliyon.2024.e33206
Received 28 March 2024; Received in revised form 17 June 2024; Accepted 17 June 2024
Available online 20 June 2024

1. Introduction

The latest statistics report from the American Cancer Society shows that the number of new cancer cases in the United States is expected to exceed 2 million by 2024 [1]. For men, the top 10 most common cancers were prostate cancer, lung cancer, colorectal cancer, bladder cancer, melanoma, kidney cancer, non-Hodgkin lymphoma, oral cancer, leukemia and pancreatic cancer. For women, the top 10 most common cancers were breast cancer, lung cancer, colorectal cancer, cervical cancer, melanoma, non-Hodgkin lymphoma, pancreatic cancer, thyroid cancer, kidney cancer and leukemia. Cancer deaths in the United States are projected to be 611,720 in 2024, with lung, colorectal and pancreatic cancers accounting for the largest number of deaths [1]. In recent years, with the advancement of anti-tumor treatments such as targeted therapy and immunotherapy, many cancer patients have benefited from them [2]. However, the mortality rate of cancer patients remains high due to tumor metastasis, drug resistance and lack of effective early diagnosis.

Hypoxia is a typical feature of many solid tumors, and the hypoxia microenvironment is a key factor in tumor occurrence, malignant progression, treatment resistance and immune escape [3,4]. Existing studies have shown that the activities of EGLN (Egl-9 family hypoxia inducible factor) members EGLN1, EGLN2, and EGLN3 are not limited to HIF (Hypoxia Inducible Factor) regulation but also include the regulation of cell survival, cell cycle, proliferation, and metastasis [5]. In the present study, we systematically explored the expression profile, single-cell function, immune infiltration level, and regulatory signaling pathway of EGLN3 in pan-cancers. We also focused on the role of EGLN3 in the regulation of malignant phenotypes in lung cancer.

2. Materials and methods

2.1. Database and public platform

We obtained gene expression data, clinicopathological data, and survival data from UCSC Xena for 33 cancers present in TCGA. The UALCAN database (https://ualcan.path.uab.edu/) was used to identify differences in expression of EGLN3 in pan-cancer and normal tissues [6,7]. We also investigated the RNA expression level of EGLN3 in some tumors using the Human Protein Atlas (HPA) database (https://www.proteinatlas.org/) and determined the subcellular localization of EGLN3 through immunofluorescence microscopy [8]. We examined the expression of EGLN3 in different single-cell types in the HPA database. At the same time, we also used the EGAD00001007030 dataset (https://ega-archive.org/studies/EGAS00001005115) (n = 18) in Single Cell Portal database (https://singlecell.broadinstitute.org/single_cell) to investigate the expression of EGLN3 in a variety of tumor types, such as breast cancer, prostate cancer, and melanoma [9]. In addition, we used the GSE148071 dataset (n = 42) from the Tumor Immune Single-cell Hub 2 (TISCH2) database (http://tisch.comp-genomics.org/) to investigate the expression level of EGLN3 in non-small cell lung cancer (NSCLC) [10,11]. The CancerSEA database (http://biocc.hrbmu.edu.cn/CancerSEA/) was used for single-cell function analysis of EGLN3 in pan-cancer [12]. We used the TISIDB database (http://cis.hku.hk/TISIDB/) to detect the expression of EGLN3 in different molecular types and immune types in pan-cancer [13]. The TIMER2.0 database (http://timer.cistrome.org/) was used to analyze the tumor immunoinfiltration of EGLN3 in pan-cancer [14]. The co-expression network and KEGG enrichment analysis of EGLN3 in LUAD and LUSC were performed using the LinkedOmics database (http://linkedomics.org/login.php) [15]. In the "LinkFinder" module, the volcano plots and heat maps show genes that are positively/negatively associated with EGLN3. In the "LinkInterpreter" module, EGLN3-enriched KEGG pathways are represented by bubble maps.

2.2. Cell culture and transfection

The human lung cancer cell lines A549 and NCI–H1650 were obtained from the Cell Bank of Chinese Academy of Sciences (Shanghai, China), and cultured in RPMI-1640 medium containing 10 % fetal bovine serum at 37 °C and 5 % CO_2. EGLN3-targeted siRNA (siRNA-EGLN3) and negative control scrambled siRNA (si-NC) were synthesized by Guangzhou RiboBio Company. Apoptosis and gene expression were measured 48 h after transfection with 50 nM siRNA.

2.3. RNA extraction and real-time quantitative PCR

An extraction of total RNA was performed using TRIzol® reagent (Invitrogen; Thermo Fisher Scientific Inc.). To perform reverse transcription, we used PrimeScript™ RT reagent kit (Takara Bio, Inc.), and to perform RT-qPCR, we used SYBR Green PCR kit (Takara Bio, Inc.). We used the following primers: GAPDH forward, 5′-CCCATCACCATCTTCCAGGAG-3′ and reverse, 5′-GTTGTCATGGATGACCTTGGC-3'; EGLN3 forward, 5′- CTGGGCAAATACTACGTCAAGG-3′ and reverse, 5′- GACCATCACCGTTGGGGTT-3'. GAPDH was the internal reference gene, and data were calculated using the $2^{-\Delta\Delta CT}$ method.

2.4. Western blotting

We extracted protein from A549 and NCI–H1650 cells using RIPA lysis buffer (Abcam). Proteins were separated by 10 % SDS–PAGE, transferred to nitrocellulose membranes, and then incubated at room temperature for 2 h with blocking solution (5 % skimmed milk). Incubation of the primary antibody with the samples was performed at 4 °C overnight, followed by incubation of the secondary antibody at room temperature for 2 h. The primary antibodies used included: GAPDH (Absin, abs132004, 1: 3000), EGLN3 (Abcam, ab184714, 1: 5000), Bax (Bioworld Technology, MB66266, 1:1000), and Bcl-2 (Bioworld Technology, MB62589, 1:2000). GAPDH was

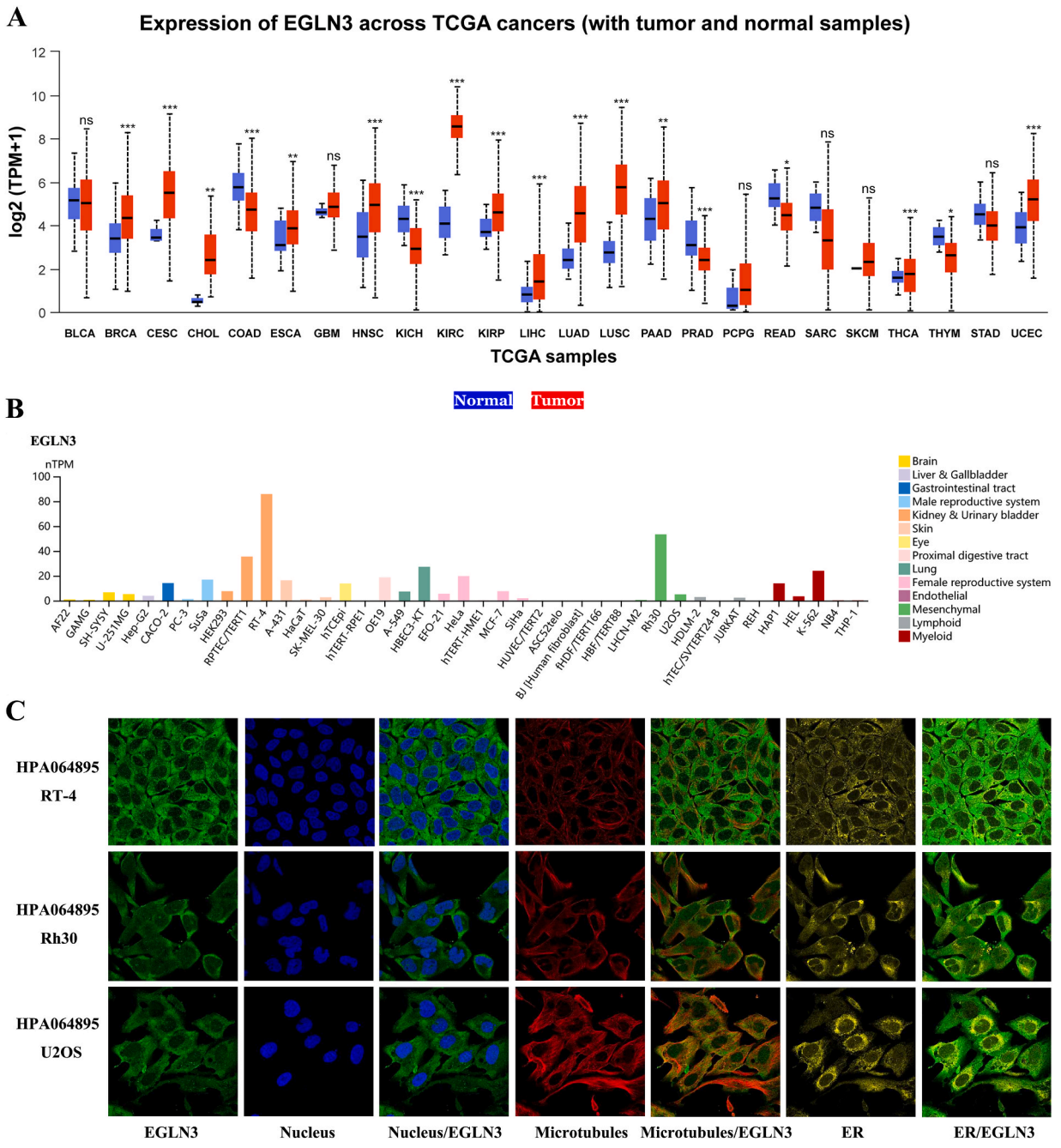

Fig. 1. The expression landscape of EGLN3 in pan-cancer. (A) The expression of EGLN3 across TCGA cancers. (B) The expression levels of EGLN3 in multiple tumor cell lines. (C) The subcellular immunofluorescence staining of EGLN3 protein, nucleus, endoplasmic reticulum (ER), microtubules and the merged images in RT-4, Rh30, and U2OS cell lines. (*p < 0.05, **p < 0.01, ***p < 0.001).

the internal parameter; anti-rabbit IgG, HRP-linked Antibody (Cell Signaling Technology, 7074P2, 1: 1000). ECL luminescence reagent (Absin, abs920) was used for protein visualization.

2.5. Flow cytometry analysis

In order to detect cell apoptosis, the Annexin V-APC/PI Apoptosis Detection Kit from KeyGEN (KGA1030-1007) was used. Apoptosis was assessed using flow cytometry (CytoFLEX Flow Cytometer, Beckman Coulter, Inc.).

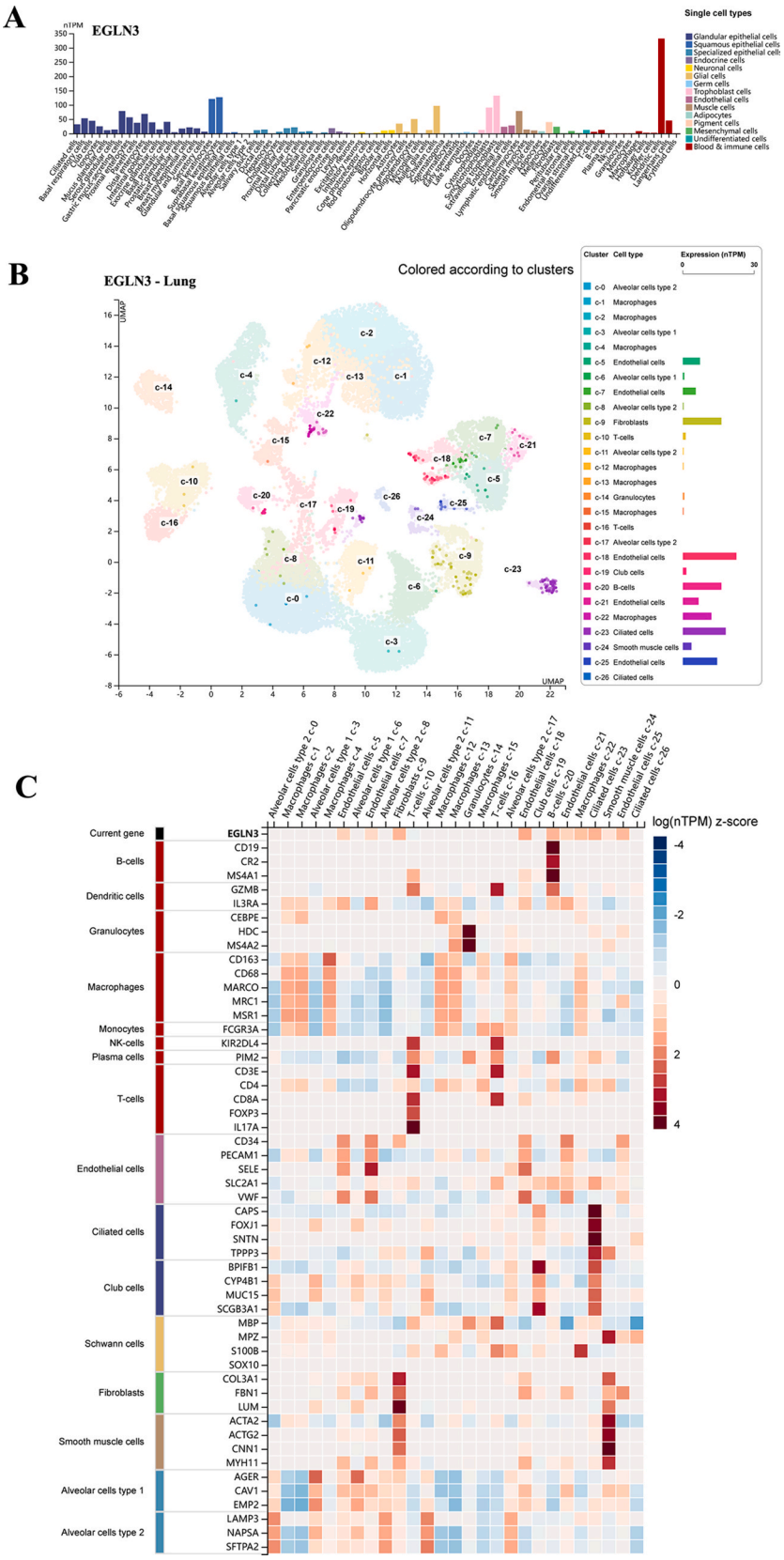

(caption on next page)

Fig. 2. Single-cell expression landscape of EGLN3 in HPA database. (A) The expression of EGLN3 in different single-cell types. (B) UMAP shows the cell clusters in the lung. (C) The heat map shows expression of EGLN3 and well-known cell type markers in the different single-cell type clusters of lung tissue. The panel on the left shows which cell type each marker is associated with. Color-coding is based on cell type groups, each consisting of cell types with functional features in common. (For interpretation of the references to color in this figure legend, the reader is referred to the Web version of this article.)

2.6. Cell proliferation assay (CCK8)

A549 and NCI–H1650 cells were seeded in 96-well plates and cell proliferation was examined by Cell Counting Kit-8 (CCK8) (Abiowell, AWC0114a) according to the manufacturer's instruction.

2.7. Transwell migration assay

We performed migration experiments using 24-well transwell chambers with 8-μm aperture (Corning, Inc.). A cell density of 6×10^5 cells/mL was adjusted after cell collection and resuspension in serum-free RPMI 1640 medium. We inoculated 100 μL of cell suspension into the upper chamber and 500 μL of RPMI-1640 medium containing 10 % FBS into the lower chamber. Incubation at 37 °C for 24 h and staining at room temperature with 0.1 % crystal violet for 20 min were the procedures. Using a light microscope (magnification, ×100), three fields were randomly selected to photograph, and the number of migrated cells was manually counted.

3. Results

3.1. Expression landscape of EGLN3 in pan-cancer

To investigate the expression of EGLN3 in pan-cancer, we examined the expression of EGLN3 in tumor tissues and cell lines. Compared with normal tissues, EGLN3 is highly expressed in a variety of tumors, such as BRCA ($P < 0.001$), CESC ($P < 0.001$), CHOL ($P < 0.01$), ESCA ($P < 0.01$), HNSC ($P < 0.001$), KIRC ($P < 0.001$), KIRP ($P < 0.001$), LIHC ($P < 0.001$), LUAD ($P < 0.001$), LUSC ($P < 0.001$), PAAD ($P < 0.01$), and UCEC ($P < 0.001$) (Fig. 1A). Subsequently, we detected EGLN3 expression levels in a variety of tumor cell lines. The results showed that EGLN3 was highly expressed in RT-4, Rh30, RPTEC/TERT1, A431, SuSa, CACO2, OE19, A549, HBEC3-KT, HeLa, HAP1, and K562 (Fig. 1B). In addition, subcellular localization of EGLN3 was performed by immunofluorescence staining in RT-4, Rh30 and U2OS cells based on HPA database. EGLN3 was mainly localized to the cytosol (Fig. 1C).

3.2. Single-cell sequencing analysis of EGLN3

RNA single-cell type specific analysis demonstrated that EGLN3 expression was enhanced in dendritic cells, extravillous trophoblasts, suprabasal keratinocytes, basal keratinocytes and other cell types (Fig. 2A). Scatter plot showed the expression of EGLN3 in different cell clusters in the lung, with high expression mainly concentrated in fibroblasts, endothelial cells, B-cells, macrophages (Fig. 2B). The heat map shows expression of EGLN3 and well-known cell type markers in the different single-cell type clusters of lung tissue (Fig. 2C). For example, fibroblast markers COL3A1 (z-score = 3.07), FBN1 (z-score = 2.35), and LUM (z-score = 3.88) showed high expression. B-cell markers CD19 (z-score = 4.16), CR2 (z-score = 3.19), and MS4A1 (z-score = 4.11) showed the same trend.

The Single Cell Porta database was used to investigate the expression of EGLN3 in different cell subsets in breast cancer, prostate cancer, and melanoma (Fig. 3). Next, the NSCLC-GSE148071 single-cell dataset containing 42 patients with primary cancer was used to investigate the expression of EGLN3 in different cell subsets in NSCLC (Fig. 4). We analyzed the NSCLC-GSE148071 dataset, and Fig. 4A–C showed that it was divided into 10 cell types, among which malignant cells (48,118), mononuclear/macrophages (14,078) and fibroblasts (4792) were the most abundant. We also investigated the distribution of EGLN3 in different cell types (Fig. 4D). Heat maps show upregulated immune-related gene sets mainly enriched in fibroblasts and mononuclear/macrophages (Fig. 4E). Cell-to-cell interaction (CCI) analysis revealed that EGLN3-fibroblasts mainly interact with malignant cells, alveolar, mononuclear/macrophages (Fig. 4F) and that EGLN3-macrophages mainly interact with fibroblasts (Fig. 4G). To explore the role of EGLN3 in NSCLC, we performed GSEA analysis on the scRNA-seq data from the GSE148071 dataset and found that, compared to other identified cell types, The hallmark_hypoxia, hallmark_apoptosis, and hallmark_epithelial-mesenchymal transition gene sets were specifically enriched in NSCLC (Fig. 4H–J).

To further explore the role of EGLN3 in tumors, we investigated the function of EGLN3 at the single-cell level using CancerSEA (Fig. 5). The results suggest that EGLN3 is associated with hypoxia in a variety of tumors, including GBM, glioma, LUAD, NSCLC, RCC, BRCA, PC, HNSCC, and OV. In LUAD, EGLN3 was positively correlated with angiogenesis, apoptosis, hypoxia, inflammation, metastasis, and stemness. EGLN3 was positively associated with angiogenesis, DNA repair, hypoxia, inflammation, invasion, metastasis and stemness of PC. However, EGLN3 was negatively associated with apoptosis, DNA damage repair, hypoxia, invasion, metastasis, and stemness in UM. These results suggest that EGLN3 may be involved in the regulation of tumor malignant process, which needs to be verified *in vitro* and in vivo.

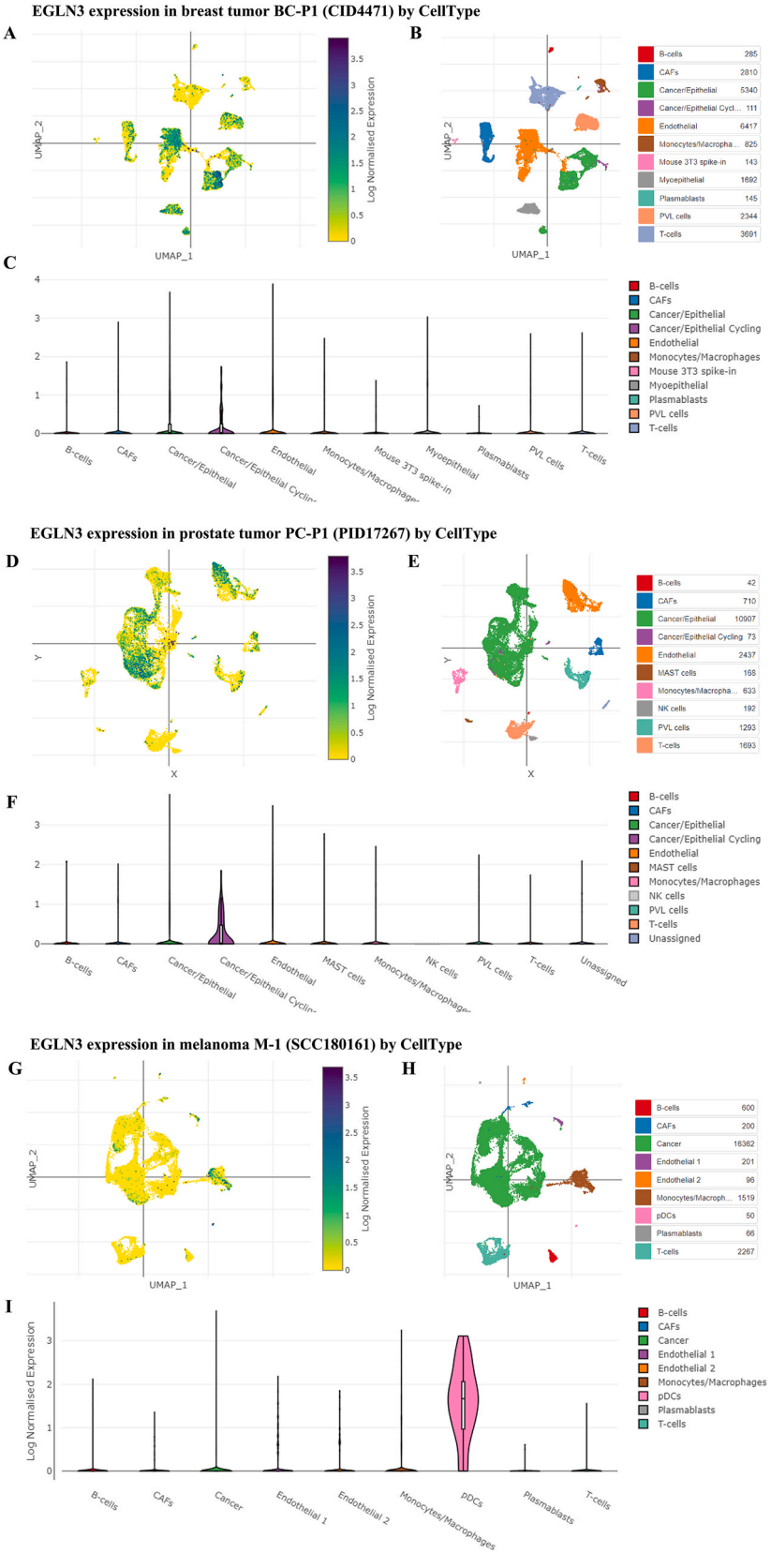

(caption on next page)

Fig. 3. Single-cell expression analysis of EGLN3 in tumors. (A–C) Breast cancer. (D–F) Prostate cancer. (G–I) Melanoma.

3.3. Immune aspects of EGLN3 in tumor microenvironment

It is well known that the tumor immune microenvironment plays an important role in the malignant process of tumors. The violin map revealed that EGLN3 expression in multiple tumors was significantly correlated with immune and molecular subtypes (Fig. 6). The expression of EGLN3 in molecular subtypes of BRCA (P = 4.76e-14), COAD (P = 6.06e-09), LGG (P = 8.97e-07), LIHC (P = 2.44e-07), LUSC (P = 3.28e-05), PCPG (P = 7.1e-04), PRAD (P = 1.25e-06), SKCM (P = 4.78e-07), and UCEC (P = 6.95e-04) was all significantly different (Fig. 6A). EGLN3 expression showed significant correlation with immune subtypes in KIRC (P = 5.41e-04), LGG (P = 1.23e-09), LIHC (P = 5.51e-09), LUAD (P = 4.33e-16), LUSC (P = 4.06e-04), PAAD (P = 1.89e-04), and PRAD (P = 1.76e-05) (Fig. 6B).

The correlation between EGLN3 expression and tumor immune cell infiltration was analyzed using TIMER 2.0 database. Spearman correlation analysis was used to investigate the association between EGLN3 and immune infiltration levels of immune cells including macrophages, neutrophils, myeloid dendritic cells, B cells, regulatory T cells (Tregs), $CD8^+$ T cells, endothelial cells, mast cells, monocytes, natural killer (NK) cells, and $CD4^+$ T cells in pan-cancer (Fig. 7). We focused on tumor-associated fibroblasts (CAFs). Based on four algorithms: EPIC, MCPCOUNTER, XCELL, and TIDE, it was suggested that EGLN3 expression is positively correlated with infiltration by CAFs in BRCA (Rho = 0.322, P = 1.92e-25), BRCA-Basal (Rho = 0.302, P = 5.19e-05), BRCA-LumA (Rho = 0.309, P = 7.27e-13), BRCA-LumB (Rho = 0.376, P = 7.37e-08), CHOL (Rho = 0.491, P = 2.76e-03), LIHC (Rho = 0.396, P = 2.20e-14), PCPG (Rho = 0.401, P = 7.78e-08), PRAD (Rho = 0.366, P = 1.23e-14), TGCT (Rho = 0.447, P = 1.43e-08) and THCA (Rho = 0.561, P = 7.07e-42). EGLN3 was negatively correlated with immune cell infiltration in THYM (Rho = −0.613, P = 3.45e-13) (Fig. 8). Based on single-cell sequencing and immunoinfiltration analysis, we preliminarily concluded that EGLN3 is associated with tumor immunity, especially CAFs and macrophages. CAFs are the most abundant cell types in the tumor microenvironment and are the center of cross-

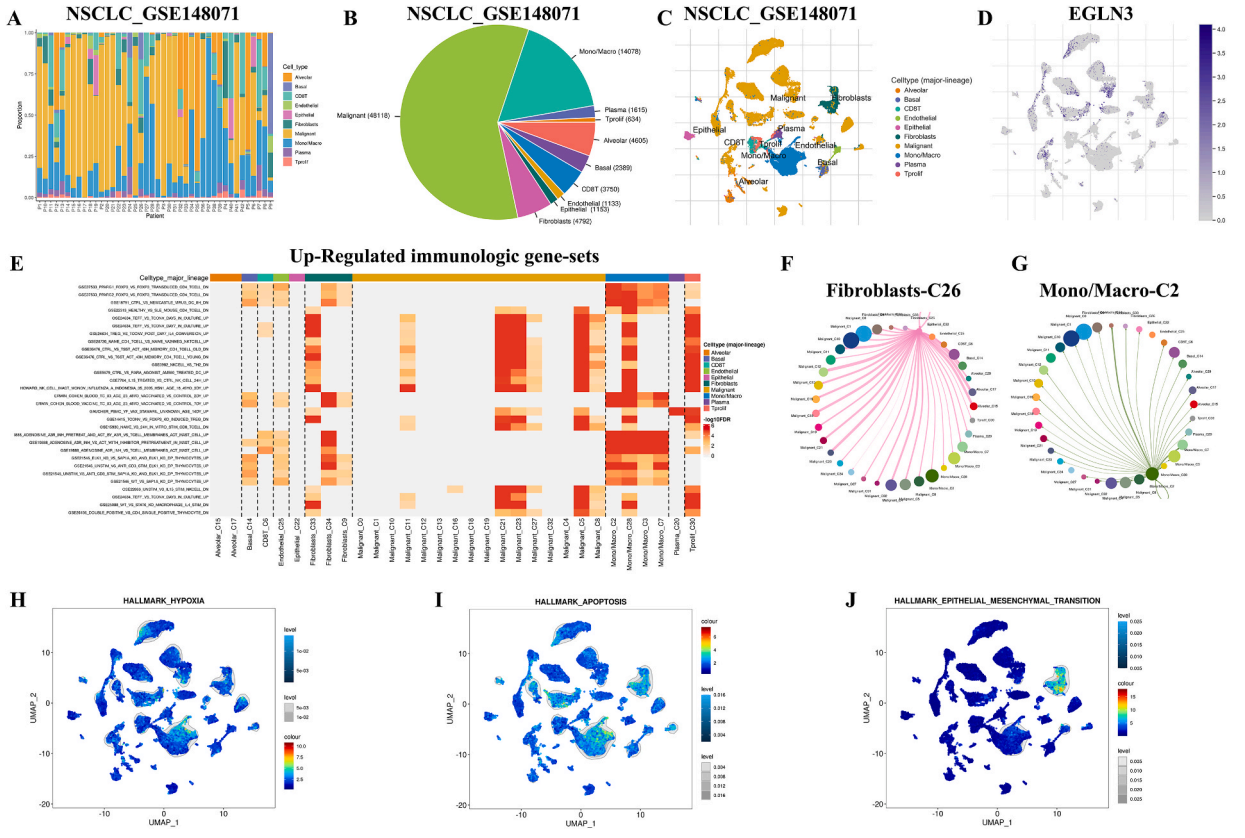

Fig. 4. Single-cell expression analysis of EGLN3 in NSCLC based on scRNA-seq. (A, B) The cell subsets distribution and TME differences in 42 NSCLC patients in GSE148071 dataset. (C) The identified cell types in NSCLC tissues based on the GSE148071 dataset. (D) The expression levels of EGLN3 in the identified cell types in NSCLC tissues based on the GSE148071 dataset. (E) The up-regulated immumologic gene-sets in NSCLC based on the GSE148071 dataset. (F) The interactions between EGLN3+CAFs and other cells based on the GSE148071 dataset. (G) The interactions between EGLN3+macrophages and other cells based on the GSE148071 dataset. (H) The enrichment of the HALLMARK_hypoxia gene-set in identified cell types based on the GSE148071 scRNA-seq data. (I) The enrichment of the HALLMARK_apoptosis gene-set in identified cell types based on the GSE148071 scRNA-seq data. (J) The enrichment of the HALLMARK_epithelial mesenchymal transition gene-set in identified cell types based on the GSE148071 scRNA-seq data.

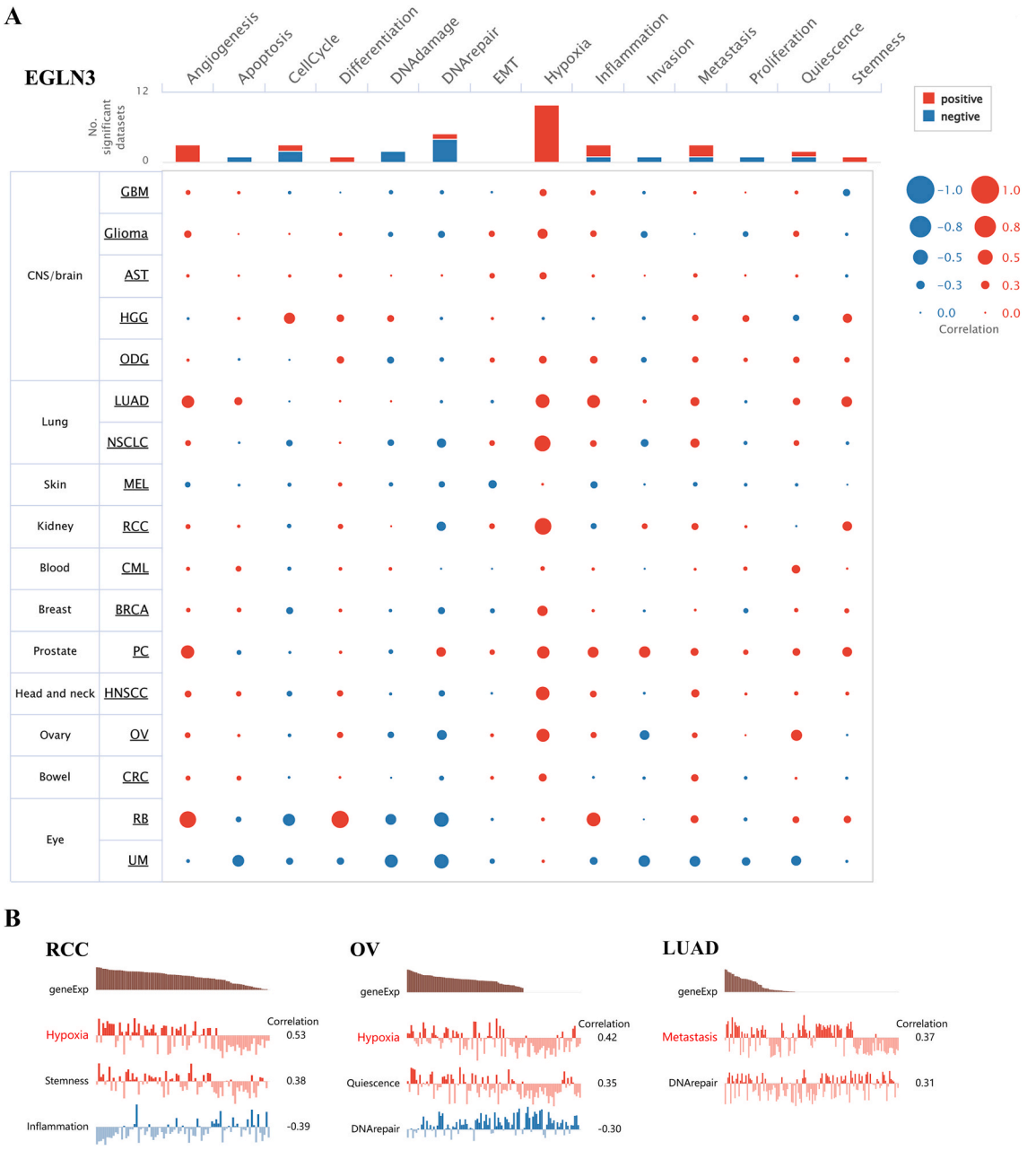

Fig. 5. The role of EGLN3 in single-cell functional analysis from the CancerSEA database. (A) Functional status of EGLN3 in different human cancers. (B) Correlation analysis between functional status and EGLN3 in RCC, OV, and LUAD. (*p < 0.05, **p < 0.01, ***p < 0.001).

communication between various cells in the tumor stroma. Targeting CAFs may become a new anti-tumor strategy.

3.4. EGLN3 co-expression network and pathway analysis in NSCLC

To investigate the molecular function of EGLN3, we performed gene network and pathway analysis. In LUAD, 6115 genes (red dots) were positively associated with EGLN3 and 4798 genes (green dots) were negatively associated with EGLN3 ($P < 0.05$) (Fig. 9A). There were 3190 genes positively correlated with EGLN3 and 4873 genes negatively correlated with EGLN3 in LUSC ($P < 0.05$) (Fig. 9D). The top 50 genes that were positively (Fig. 9B–E) or negatively (Fig. 9C–F) correlated with EGLN3 were further shown by heat map. Moreover, KEGG pathway analysis suggested that proteasome ($P < 0.001$), cell cycle ($P < 0.001$), DNA replication ($P < 0.001$), spliceosome ($P < 0.01$), TNF signaling pathway ($P < 0.01$), oxidative phosphorylation ($P < 0.01$), ECM-receptor interaction ($P < 0.01$), RNA transport ($P < 0.05$), protein export ($P < 0.05$), and IL-17 signaling pathway ($P < 0.05$) were enriched in LUAD (Fig. 10A). In

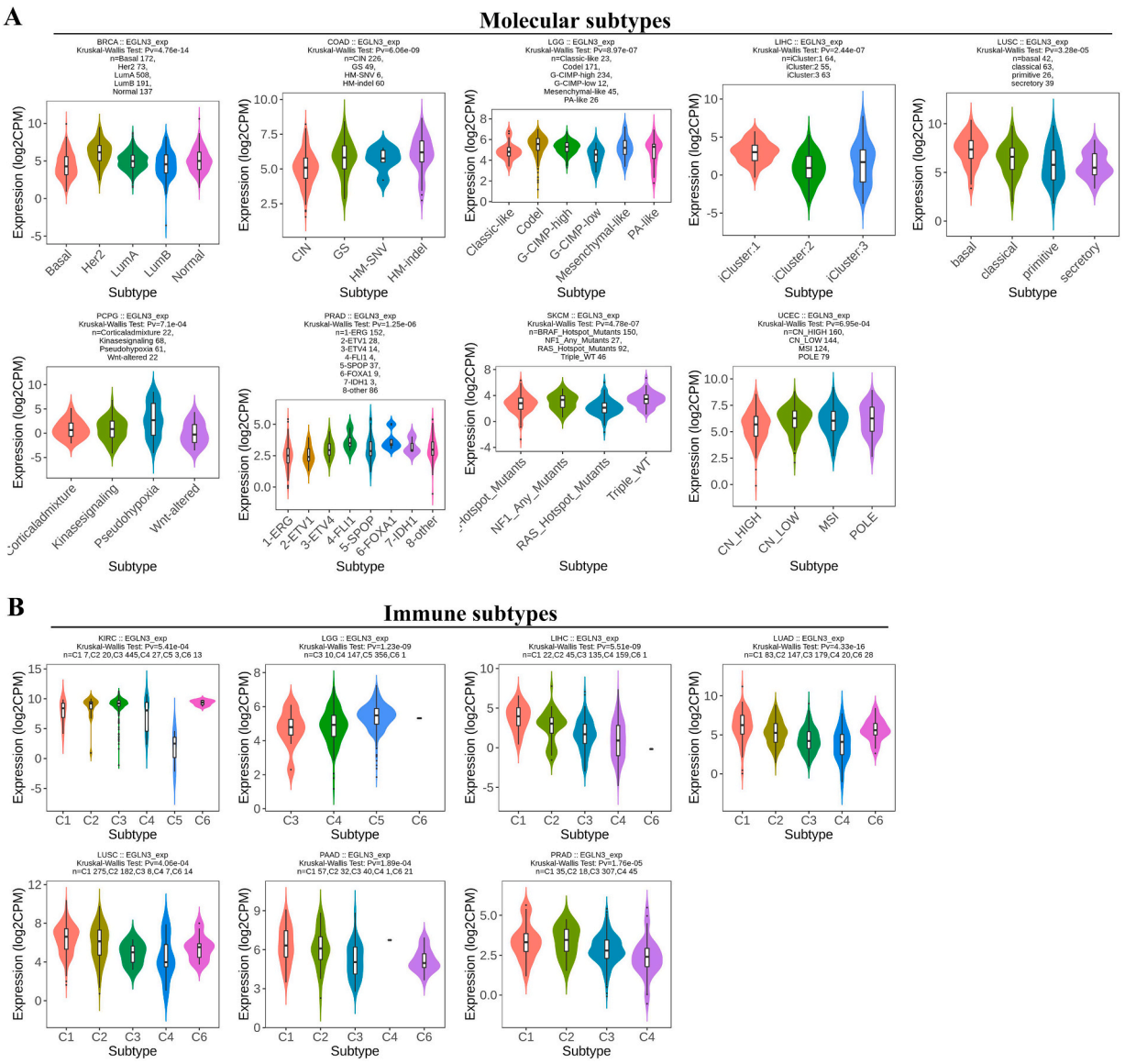

Fig. 6. The correlation between EGLN3 expression and immune subtypes and molecular subtypes in pan-cancer. (A) Expression levels of EGLN3 in diferent molecular subtypes. (B) Expression levels of EGLN3 in diferent immune subtypes. C1 (wound healing); C2 (IFN-gamma dominant); C3 (infammatory); C4 (lymphocyte depleted); C5 (immunologically quiet); C6 (TGF-b dominant).

LUSC, the top 10 enriched signaling pathways include focal adhesion ($P < 0.001$), HIF-1 signaling pathway ($P < 0.001$), fructose and mannose metabolism ($P < 0.001$), ECM-receptor interaction ($P < 0.001$), glycolysis/gluconeogenesis ($P < 0.001$), PI3K-Akt signaling pathway ($P < 0.001$), IL-17 signaling pathway ($P < 0.001$), TNF signaling pathway ($P < 0.001$), central carbon metabolism in cancer ($P < 0.01$), and pathways in cancer ($P < 0.01$) (Fig. 10B).

3.5. *EGLN3 affects the malignant progression of NSCLC cells in vitro*

EGLN3 was significantly overexpressed in LUAD (Fig. 11A) and associated with poor prognosis in patients (Fig. 11B). After reviewing a large number of literatures, it was found that the biological function of this gene in LUAD was rarely reported. Here, we examined the effects of EGLN3 on tumor proliferation, migration, and apoptosis in A549 and NCI–H1650 cells. Compared with the control group (si-NC), the expression level of EGLN3 in si-EGLN3 group was significantly down-regulated (Fig. 11C). Functional experiments revealed that EGLN3 knockdown could inhibit cell proliferation, migration, and promote cell apoptosis (Fig. 11D–F). In addition, we found that Bax expression was up-regulated and Bcl-2 expression was down-regulated in the si-EGLN3 group (Fig. 11G). Taken together, as a potential oncogene, EGLN3 is involved in the regulation of tumor malignant process, especially tumor cell

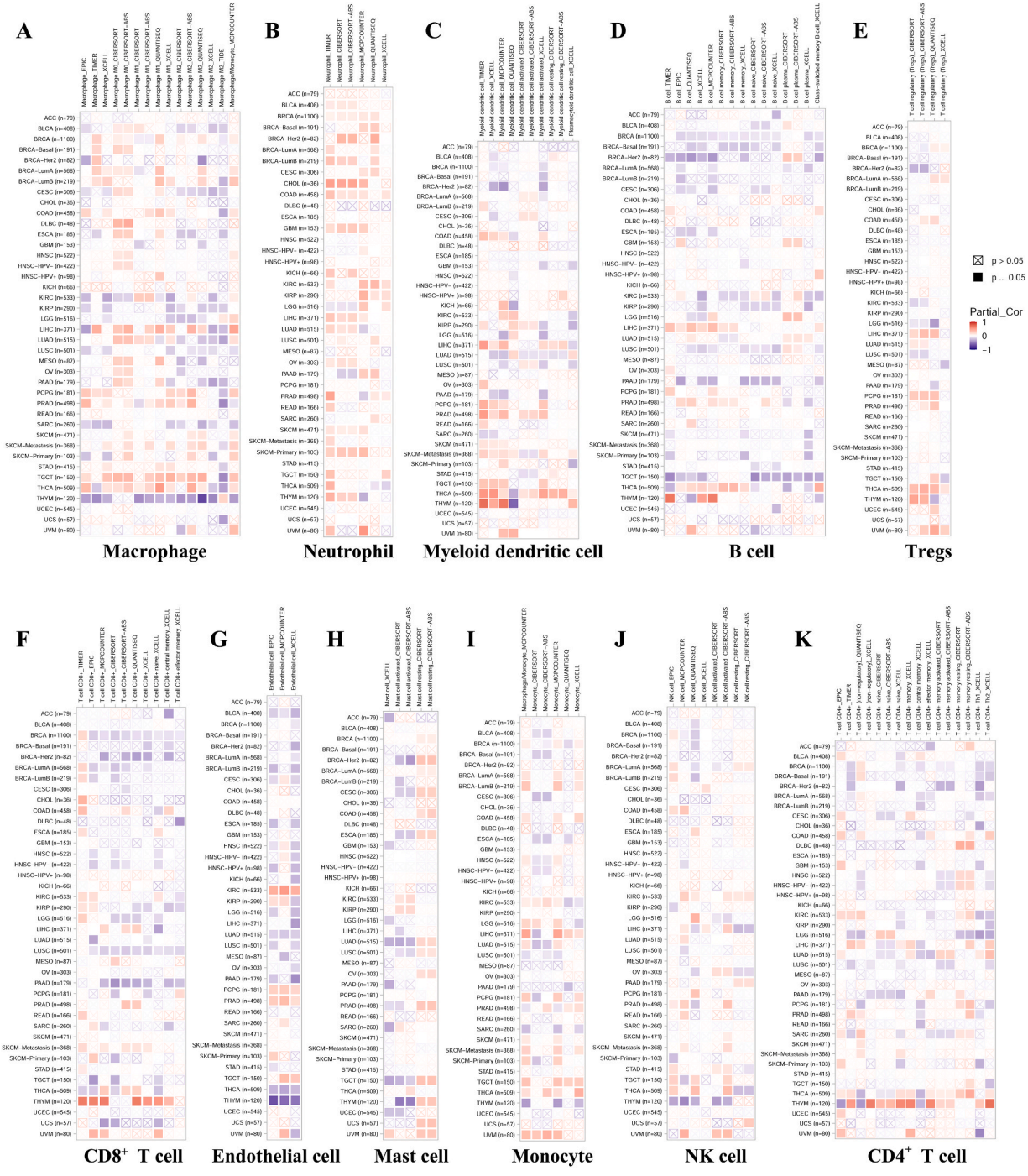

Fig. 7. Correlation analysis between EGLN3 expression and immune infiltration of various immune cells in pan-cancer. (A) Macrophage. (B) Neutrophil. (C) Myeloid dendritic cell. (D) B cell. (E) Tregs. (F) $CD8^+$ T cell. (G) Endothelial cell. (H) Mast cell. (I) Monocyte. (J) NK cell. (K) $CD4^+$ T cell.

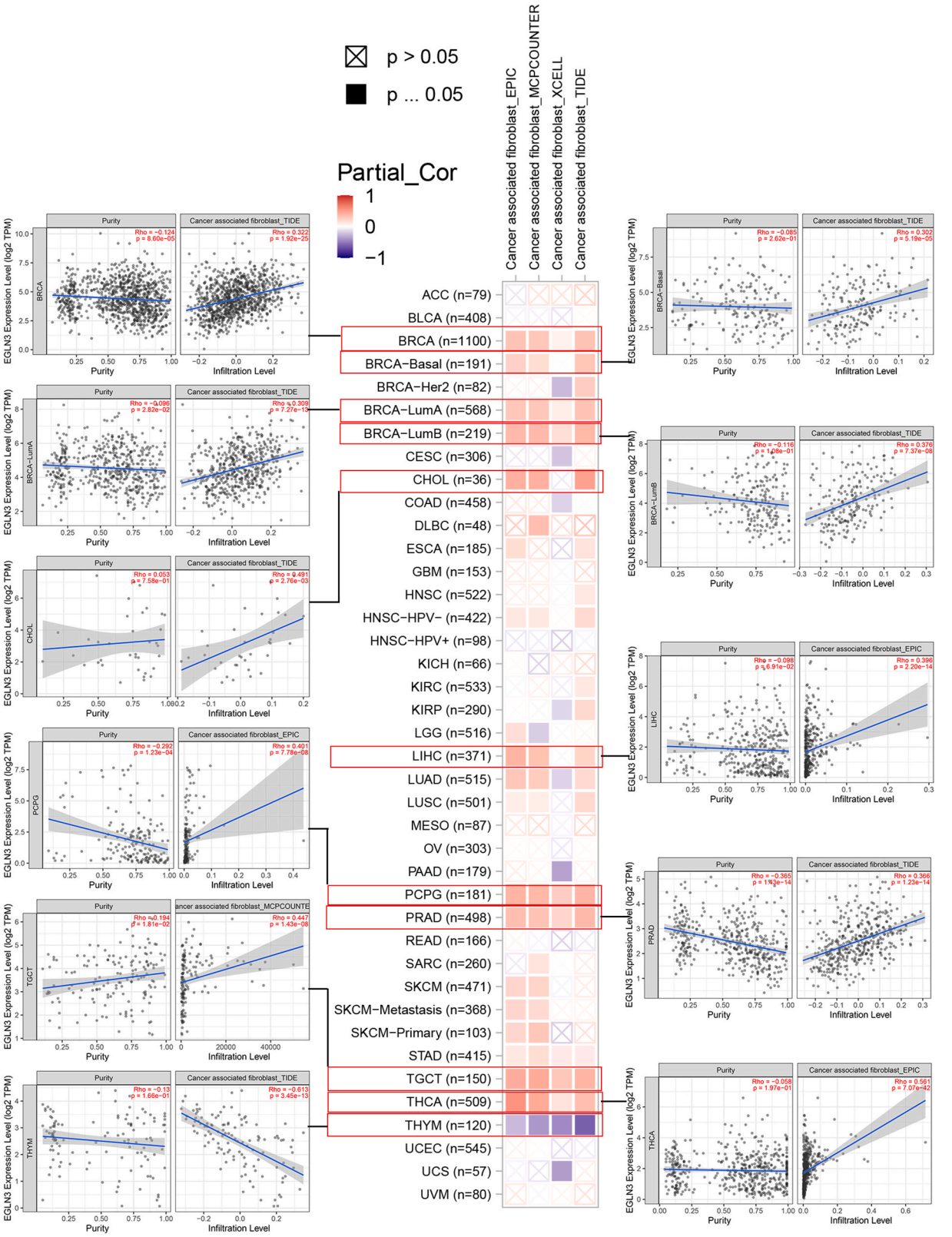

Fig. 8. Correlation analysis between EGLN3 expression and immune infiltration of cancer-associated fibroblasts (CAFs) in pan-cancer. P value less than 0.05 is considered statistically significant.

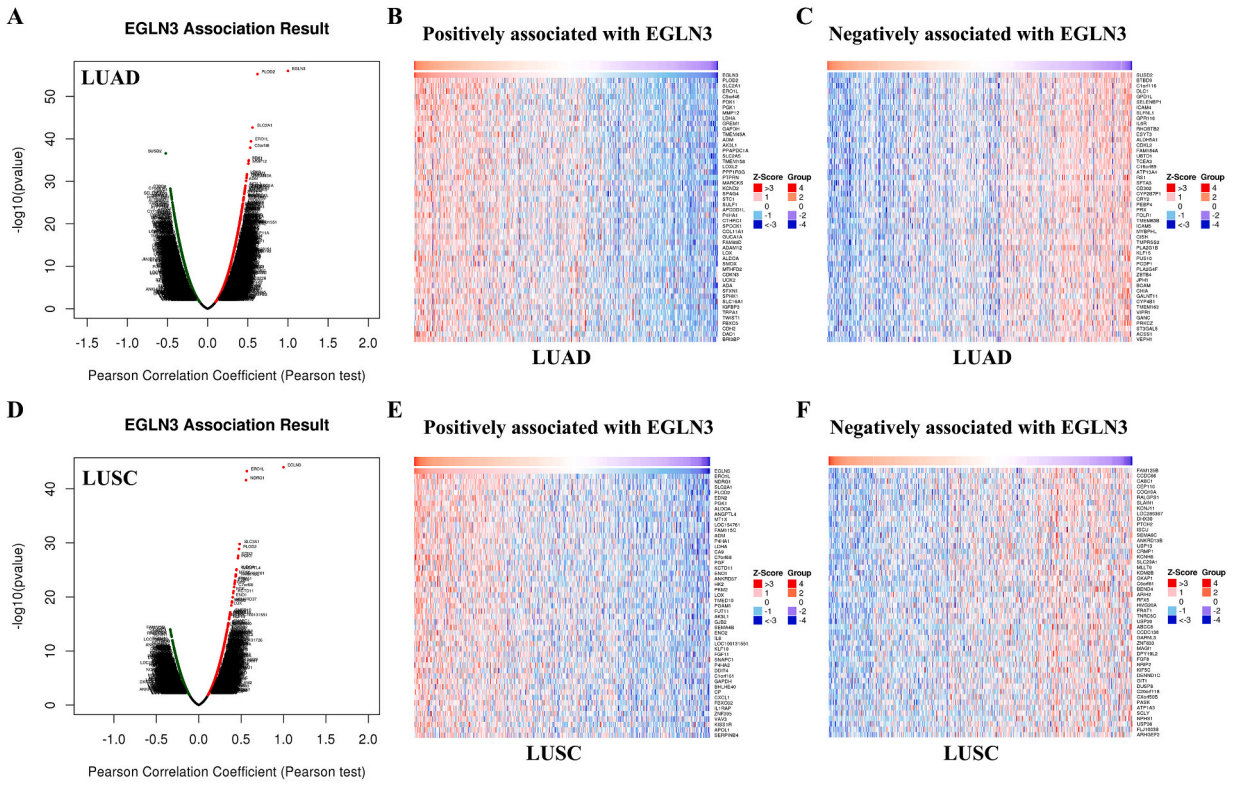

Fig. 9. EGLN3 co-expression networks in NSCLC. (A, D) Te volcano plot of EGLN3 co-expression genes. Red dots represent genes that are positively associated with EGLN3 and green dots represent genes that are negatively associated with EGLN3. Heat maps showed the top 50 positively (B, E) and negatively (C, F) co-expressed genes of EGLN3 in NSCLC. Red squares represent positive co-expressed genes and blue squares represent negative co-expressed genes. (For interpretation of the references to color in this figure legend, the reader is referred to the Web version of this article.)

apoptosis.

4. Discussion

EGLN3 is an important member of the EGLN family, and its main function is to regulate HIF factors, while participating in the regulation of tumor microenvironment and tumor malignant process [5,16–18]. Our study found that EGLN3 is significantly over-expressed in LUAD and is associated with poor prognosis. Functional experiments also revealed that EGLN3 knockdown could inhibit cell proliferation and migration, and promote cell apoptosis. However, this study has not yet elucidated the molecular mechanism by which EGLN3 promotes tumor apoptosis, which we will address in the future.

Anoxic microenvironment is a common feature of most solid tumors. Hypoxia has a profound influence on the biological behavior and malignant phenotype of cancer cells, mediates the effects of cancer chemotherapy, radiotherapy and immunotherapy through complex mechanisms, and is closely related to the poor prognosis of various cancer patients [19–21]. Previous studies have shown that drugs targeting key genes associated with hypoxia, as well as drugs targeting hypoxia-inducing factors and downstream targets can be used for visualization and quantitative analysis of tumor hypoxia and antitumor activity. However, the relationship between hypoxia and cancer is an area of research that needs to be further explored. By single-cell functional analysis, we found that EGLN3 was positively correlated with hypoxia in malignant tumors, especially in LUAD, NSCLC, RCC, HNSCC, and OV. EGLN3 may serve as a novel tumor therapeutic target by regulating hypoxic-related signaling pathways.

Macrophages are the largest number of immune cells in the tumor microenvironment except for tumor cells. Due to their phagocytosis, they can destroy tumor cells at an early stage. However, under the domestication of the tumor microenvironment, macrophages are gradually polarized into tumor-related macrophages with M2 phenotype, which promote tumor growth, invasion and metastatic spread by inhibiting immunity and inducing neovascularization [22–25]. Previous lung cancer studies have shown that tumor-associated macrophages (TAMs) exhibit a pro-inflammatory and anti-tumor phenotype (M1 type) in the early stage of lung cancer, and gradually exhibit an anti-inflammatory and pro-tumor phenotype (M2 type) during the progression of lung cancer. Understanding the immunoinfiltration of macrophages in the tumor microenvironment is important for developing new cancer immunotherapy strategies. Tumor-associated fibroblast (CAF) is an important cell type in the tumor microenvironment, which plays an indispensable role in promoting tumor growth [26–28]. It can promote cancer cell growth, inhibit tumor immune response, reshape ECM, influence tumor cell drug resistance and promote angiogenesis to promote tumor progression and metastasis [29–31]. Therefore,

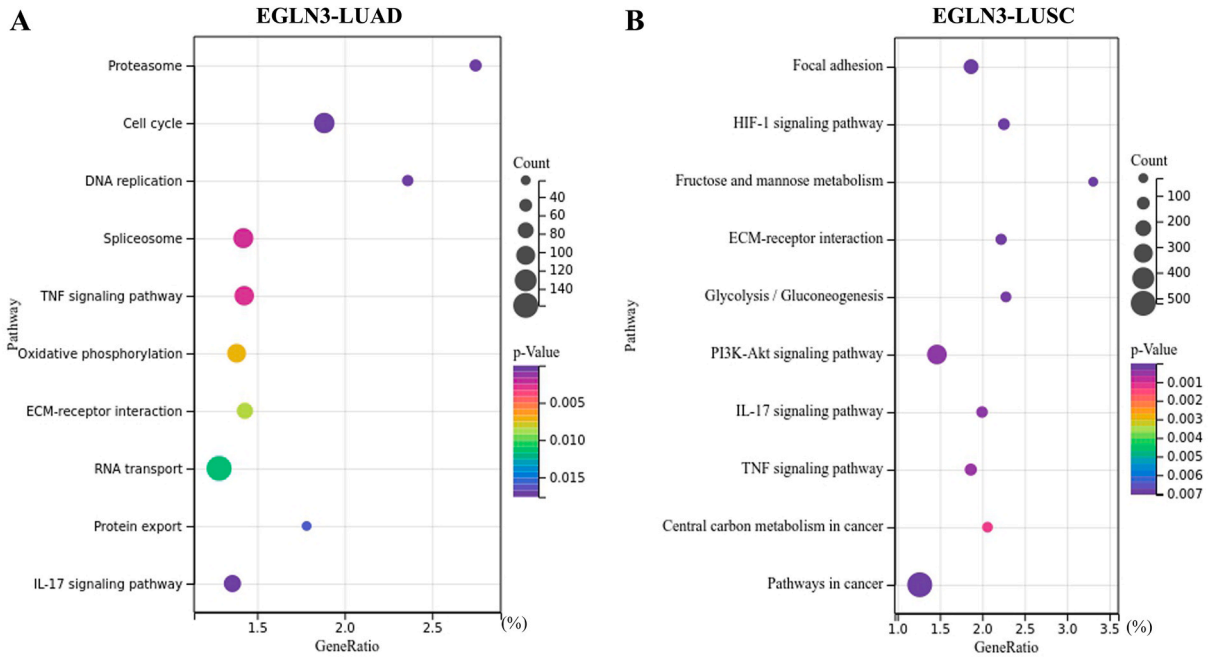

Fig. 10. The signaling pathway analysis of EGLN3 in NSCLC. (A) LUAD. (B) LUSC. Y-axis represents the enriched signaling pathway. X-axis: GeneRatio is the ratio of the number of genes enriched to the target pathway from the target gene list to the total genes contained in the gene list. Bubble area size: the number of enriched genes. Bubble color: Enrichment significance, which is the size of the p-Value. (For interpretation of the references to color in this figure legend, the reader is referred to the Web version of this article.)

targeting CAF has become a new anti-tumor therapy strategy in recent years. In this study, we found that EGLN3 is involved in the regulation of TAMs and CAFs through single-cell functional analysis and immunoinfiltration analysis. We suggest that EGLN3 may promote the malignant process of tumor by regulating the tumor immune microenvironment. In the future, we will confirm this hypothesis through in-depth in vivo and *in vitro* experiments.

In summary, we comprehensively investigated the expression pattern, single-cell function, immune infiltration level and regulated signaling pathway of EGLN3 in pan-cancer. We focused on the role of EGLN3 in the regulation of malignant phenotypes in lung cancer. We found that EGLN3 is an important hypoxia and immune-related gene that may serve as a potential target for tumor immunotherapy.

Ethics approval and consent to participate

Not applicable.

Funding

This work was supported by National Natural Science Foundation of China (No. 82104304), the Key Research Project of Hunan Provincial Department of Education (No. 23A0090), Natural Science Foundation of Hunan Province of China (No. 2022JJ40224), and Scientific Research Project of Hunan Provincial Health Commission (No. 202103021291).

CRediT authorship contribution statement

Yuan-Xiang Shi: Writing – review & editing, Writing – original draft, Project administration, Funding acquisition, Conceptualization. **Peng-Hui Dai:** Writing – review & editing, Software, Methodology, Investigation, Data curation. **Tao Chen:** Writing – review & editing, Visualization, Validation, Software, Methodology. **Jian-Hua Yan:** Writing – review & editing, Software.

Declaration of competing interest

The authors declare that they have no known competing financial interests or personal relationships that could have appeared to influence the work reported in this paper.

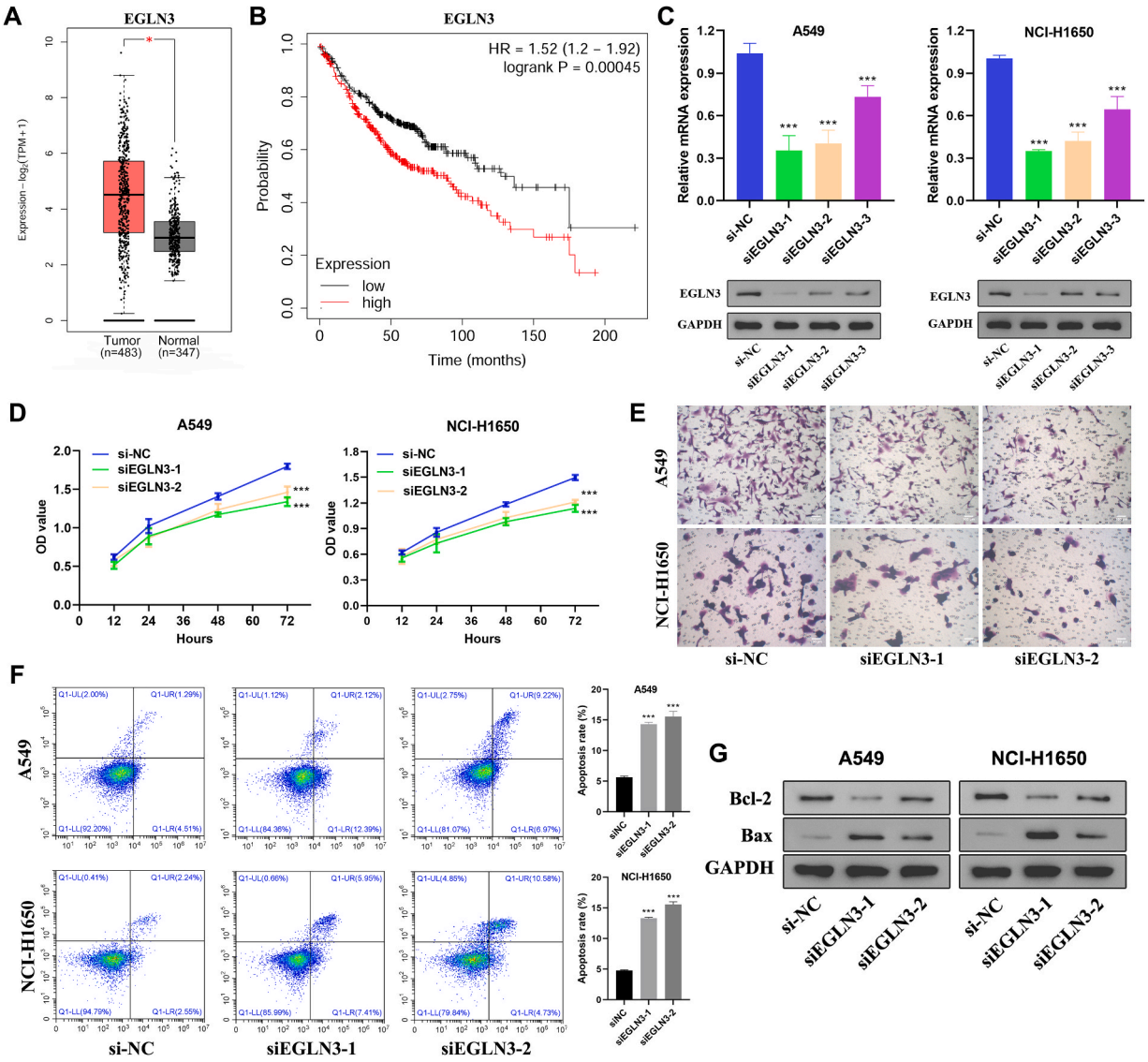

Fig. 11. EGLN3 affects the malignant progression of NSCLC cells *in vitro*. (A) The mRNA expression of EGLN3 in LUAD and normal lung tissues. (B) Survival analysis of EGLN3 in LUAD in Kaplan–Meier plotter. Overall survival (OS) was used as an indicator. (C) siRNA effectively regulated the expression of EGLN3 in the A549 and NCI–H1650 cells. mRNA and protein expression of EGLN3 were detected by RT-qPCR and western blotting, respectively. (D) CCK8 assay was used to assess cell proliferation. (E) Cell migration was assessed using the transwell assay. (F) Flow cytometry was used to verify cell apoptosis. (G) Western blot was used to detect the expression of apoptosis-related genes (Bcl-2, and Bax). *P < 0.05, **P < 0.01 and ***P < 0.001. si-NC, scrambled negative control; si, small interfering. All these experiments are compared between the experimental group and the control group.

Acknowledgements

Not applicable.

Appendix A. Supplementary data

Supplementary data to this article can be found online at https://doi.org/10.1016/j.heliyon.2024.e33206.

Abbreviations

EGLN3	Egl-9 family hypoxia-inducible factor 3
ACC	Adrenocortical carcinoma
AML	Acute myeloid leukemia
BLCA	Bladder urotelial carcinoma
BRCA	Breast invasive carcinoma
CESC	Cervical squamous cell carcinoma and endocervical adenocarcinoma
CHOL	Cholangiocarcinoma
COAD	Colorectal adenocarcinoma
DLBC	Lymphoid Neoplasm Diffuse Large B-cell Lymphoma
ESCA	Esophageal carcinoma
GBM	Glioblastoma multiforme
HNSC	Head and neck squamous cell carcinoma
KICH	Kidney Chromophobe carcinoma
KIRC	Kidney renal clear cell carcinoma
KIRP	Kidney renal papillary cell carcinoma
LGG	Brain Lower Grade Glioma
LIHC	Liver hepatocellular carcinoma
LUAD	Lung adenocarcinoma
LUSC	Lung squamous cell carcinoma
MESO	Mesothelioma
OV	Ovarian serous cystadenocarcinoma
PAAD	Pancreas adenocarcinoma
PCPG	Pheochromocytoma and paraganglioma
PRAD	Prostate adenocarcinoma
READ	Rectal adenocarcinoma
SARC	Sarcoma
SKCM	Skin cutaneous melanoma
STAD	Stomach adenocarcinoma
TGCT	Testicular Germ Cell Tumors
THCA	Thyroid carcinoma
THYM	Thymoma
UCEC	Uterine Corpus Endometrial Carcinoma
UCS	Uterine Carcinosarcoma
UVM	Uveal Melanoma

References

[1] R.L. Siegel, A.N. Giaquinto, A. Jemal, Cancer statistics, 2024, Ca - Cancer J. Clin. 74 (1) (2024) 12–49.
[2] A. Zafar, et al., Revolutionizing cancer care strategies: immunotherapy, gene therapy, and molecular targeted therapy, Mol. Biol. Rep. 51 (1) (2024) 219.
[3] R.G. Bristow, R.P. Hill, Hypoxia and metabolism. Hypoxia, DNA repair and genetic instability, Nat. Rev. Cancer 8 (3) (2008) 180–192.
[4] Y. Ye, et al., Characterization of hypoxia-associated molecular features to aid hypoxia-targeted therapy, Nat. Metab. 1 (4) (2019) 431–444.
[5] S. Strocchi, et al., The multifaceted role of EGLN family prolyl hydroxylases in cancer: going beyond HIF regulation, Oncogene 41 (29) (2022) 3665–3679.
[6] D.S. Chandrashekar, et al., UALCAN: an update to the integrated cancer data analysis platform, Neoplasia 25 (2022) 18–27.
[7] D.S. Chandrashekar, et al., UALCAN: a portal for facilitating tumor subgroup gene expression and survival analyses, Neoplasia 19 (8) (2017) 649–658.
[8] M. Uhlen, et al., A pathology atlas of the human cancer transcriptome, Science 357 (6352) (2017).
[9] S.Z. Wu, et al., Cryopreservation of human cancers conserves tumour heterogeneity for single-cell multi-omics analysis, Genome Med. 13 (1) (2021) 81.
[10] D. Sun, et al., TISCH: a comprehensive web resource enabling interactive single-cell transcriptome visualization of tumor microenvironment, Nucleic Acids Res. 49 (D1) (2021) D1420–D1430.
[11] F. Wu, et al., Single-cell profiling of tumor heterogeneity and the microenvironment in advanced non-small cell lung cancer, Nat. Commun. 12 (1) (2021) 2540.
[12] H. Yuan, et al., CancerSEA: a cancer single-cell state atlas, Nucleic Acids Res. 47 (D1) (2019) D900–D908.
[13] B. Ru, et al., TISIDB: an integrated repository portal for tumor-immune system interactions, Bioinformatics 35 (20) (2019) 4200–4202.
[14] T. Li, et al., TIMER2.0 for analysis of tumor-infiltrating immune cells, Nucleic Acids Res. 48 (W1) (2020) W509–W514.

[15] S.V. Vasaikar, et al., LinkedOmics: analyzing multi-omics data within and across 32 cancer types, Nucleic Acids Res. 46 (D1) (2018) D956–D963.
[16] Y. Jin, et al., Inactivation of EGLN3 hydroxylase facilitates Erk3 degradation via autophagy and impedes lung cancer growth, Oncogene 41 (12) (2022) 1752–1766.
[17] L. Lin, J. Cai, Circular RNA circ-EGLN3 promotes renal cell carcinoma proliferation and aggressiveness via miR-1299-mediated IRF7 activation, J. Cell. Biochem. 121 (11) (2020) 4377–4385.
[18] N. Chiba, et al., Overexpression of hydroxyproline via EGLN/HIF1A is associated with distant metastasis in pancreatic cancer, Am. J. Cancer Res. 10 (8) (2020) 2570–2581.
[19] Z. Chen, et al., Hypoxic microenvironment in cancer: molecular mechanisms and therapeutic interventions, Signal Transduct. Targeted Ther. 8 (1) (2023) 70.
[20] Z. Luo, et al., Hypoxia signaling in human health and diseases: implications and prospects for therapeutics, Signal Transduct. Targeted Ther. 7 (1) (2022) 218.
[21] R. Abou Khouzam, et al., Hypoxia as a potential inducer of immune tolerance, tumor plasticity and a driver of tumor mutational burden: impact on cancer immunotherapy, Semin. Cancer Biol. 97 (2023) 104–123.
[22] S. Chen, et al., Macrophages in immunoregulation and therapeutics, Signal Transduct. Targeted Ther. 8 (1) (2023) 207.
[23] M. Li, et al., Metabolism, metabolites, and macrophages in cancer, J. Hematol. Oncol. 16 (1) (2023) 80.
[24] L. Cassetta, J.W. Pollard, Targeting macrophages: therapeutic approaches in cancer, Nat. Rev. Drug Discov. 17 (12) (2018) 887–904.
[25] N.R. Anderson, et al., Macrophage-based approaches for cancer immunotherapy, Cancer Res. 81 (5) (2021) 1201–1208.
[26] R. Rimal, et al., Cancer-associated fibroblasts: origin, function, imaging, and therapeutic targeting, Adv. Drug Deliv. Rev. 189 (2022) 114504.
[27] E. Sahai, et al., A framework for advancing our understanding of cancer-associated fibroblasts, Nat. Rev. Cancer 20 (3) (2020) 174–186.
[28] G. Caligiuri, D.A. Tuveson, Activated fibroblasts in cancer: perspectives and challenges, Cancer Cell 41 (3) (2023) 434–449.
[29] Y. Chen, K.M. McAndrews, R. Kalluri, Clinical and therapeutic relevance of cancer-associated fibroblasts, Nat. Rev. Clin. Oncol. 18 (12) (2021) 792–804.
[30] G. Biffi, D.A. Tuveson, Diversity and biology of cancer-associated fibroblasts, Physiol. Rev. 101 (1) (2021) 147–176.
[31] M.E. Fiori, et al., Cancer-associated fibroblasts as abettors of tumor progression at the crossroads of EMT and therapy resistance, Mol. Cancer 18 (1) (2019) 70.